

# THREE-DIMENSIONAL INSPECTION OF PRINTED CIRCUIT BOARDS USING PHASE PROFILOMETRY \*

Luigi Di Stefano  
DEIS, University of Bologna  
Viale Risorgimento 2, 40136 Bologna, Italy  
e-mail: ldistefano@deis.unibo.it

Frank Boland  
EEE, University of Dublin  
Trinity College, Dublin 2, Ireland  
e-mail: fboland@ee.tcd.ie

## ABSTRACT

Reconstruction of 3D shape of the solder paste printed on SMT component pads is a major inspection task in the PCB manufacturing process. The paper reports on the use of phase profilometry for this inspection task. In phase profilometry a structured light pattern is projected onto the object and viewed by a camera. Since the imaged pattern is phase-modulated according to the topography of the object, the extraction of phase information from the image enables reconstructing the 3D shape. In this paper two phase-extraction methods, Fourier Transform Profilometry and Signal Domain Profilometry, are compared by means of simulations and experiments. Results show that the Fourier method performs better, yielding neat detection of the elevation with respect to PCB surface associated with solder paste.

## 1 INTRODUCTION

Surface Mount Technology (SMT) allows direct mounting of components onto pads on the PCB surface. In the SMT process wet solder paste is printed on the PCB corresponding to component pads. Then, after component placement, the joints between leads and pads are obtained by drying and reflowing solder paste. Since the amount and shape of solder paste on pads affects primarily the quality of joints, a highly accurate printing process is a mandatory requirement for the SMT process. In such a context, solder paste inspection, i.e the measurement of paste height and volume, is the task allowing the printing process to be controlled.

On-line solder paste inspection machines are typically based on laser profilometers. Low-cost equipment operates on a statistical basis, so as not to slow down the throughput of the production line, while 100 percent inspection system are extremely expensive [1].

Machine vision techniques based on structured light have been used effectively for 3D gauging and inspection of manufactured parts. Among structured light techniques, phase profilometry is particularly appealing due

to its simple optical arrangement and phase measuring methods have been recently experimented in the PCB inspection area for reconstructing the 3D shape of solder joints [2].

We investigated the use of phase profilometry for on-line solder paste inspection. This paper reports on the first part of the work, aimed at comparing Fourier Transform and Signal Domain Profilometry, which are the two major phase profilometry techniques.

## 2 PHASE PROFILOMETRY

In phase profilometry a periodic pattern is projected onto the object and viewed by a camera from an angularly offset position. The typical pattern is a sequence of equally spaced horizontal or vertical dark lines ( called “fringes” by analogy with Moiré contouring ), which are generated by the projection of a square wave grating ( Ronchi grating ).

It can be shown [3] that the image of the grating can be expressed as

$$g(x, y) = r(x, y) \sum_{n=-\infty}^{+\infty} A_n e^{j(2\pi n f_0 x + n \phi(x, y))}$$

where  $x$  and  $y$  are, respectively, the horizontal and vertical axis, the grating lines are vertical,  $f_0$  is the grating frequency at the image level,  $A_n$  are the Fourier coefficients of the grating,  $r(x, y)$  is the reflectivity associated with object's surface and  $\phi(x, y)$  is a known function of the object's height distribution. Hence, image rows are expressed as a summation of phase-amplitude modulated harmonics, amplitude modulation due to non-uniform reflectivity and phase modulation embodying the object's 3D shape. An example of the amplitude spectrum of an image row is shown in Figure 1 , where the frequency axis is normalized to  $f_0$  <sup>1</sup>.

Based on this principle, two major techniques aimed at extracting phase from the imaged grating have been devised. In Fourier Transform Profilometry ( FTP ) [4], [3] the phase profile associated with each image row is

\*This research has been carried out under a HCM Grant ( EUROFORM-TRTI project, contract ERBCHBGCT940696).

<sup>1</sup>Since the grating is a square wave, the spectrum contains only the odd harmonics. The low frequency spectrum is due to  $r(x, y)$ .

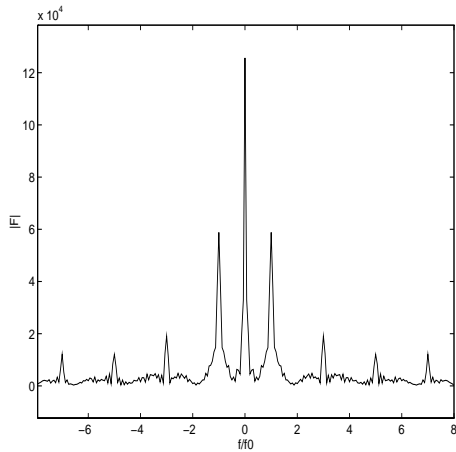


Figure 1: Spectrum of an image row.

evaluated as the angle of the analytic representation of the modulated first harmonic. This is obtained by computing the FFT of the row, filtering out all frequencies outside a narrow band centered at  $f_0$  and then computing the IFFT. In Signal Domain Profilometry (SDP) [5] each image row is multiplied by  $e^{-j2\pi f_0 x}$  so as to shift the spectrum towards the left by  $f_0$ . Thus, the phase signal associated with the first harmonic moves to low-frequency and can be extracted through a low-pass linear phase FIR filter. The phase profile is evaluated as the angle of the complex signal extracted. SDP's major purpose is to substantially reduce computing time with respect to FTP. In [5] it is estimated that, with a 9 tap FIR filter and a row size ranging from 256 to 1024 pixels, SDP is roughly three times faster than FTP. Hence, SDP is potentially more attractive than FTP for on-line solder paste inspection due to its higher speed.

### 3 SIMULATION OF PHASE PROFILOMETRY TECHNIQUES

In this section we assume a rectangular shape for the object's height profile, which is suitable to the solder paste inspection task, and simulate the projection of a 1D fringe pattern in order to compare profile reconstruction by FTP and SDP. We consider a fine and a coarse fringe pattern.

For SDP implementation we address minimax FIR filters designed by the Parks-Mc Clellan algorithm [6]<sup>2</sup>, and set the filter order to 9, so as to render SDP considerably faster than FTP. The cutoff frequency used in the design of the low-pass filter is  $f_0/2$ . Assuming uniform surface reflectivity, we subtract the mean value from the fringe image in order to get rid of the DC component. With regard to FTP, since implementation of the frequency-domain filter as a rectangular window yields ripple, we use a weighting window such as the

<sup>2</sup>The *remez()* function of MATLAB Signal Processing Toolbox is used for Parks-Mc Clellan optimal FIR filter design.

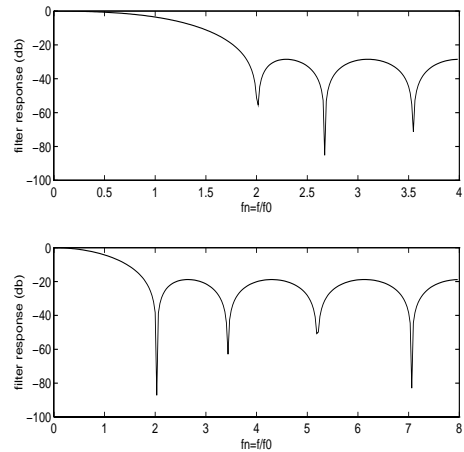


Figure 2: Designed FIR filters.

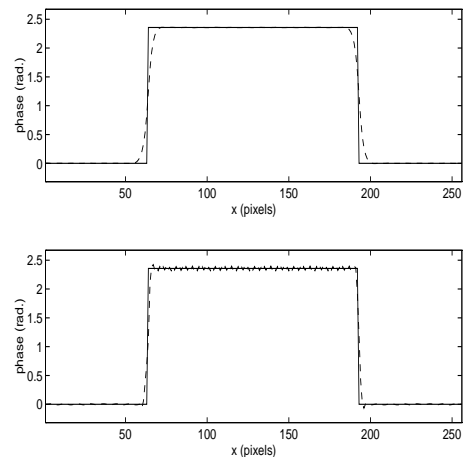


Figure 3: Profile reconstruction by FTP and SDP.

hanning window.

First, we consider the fine fringe pattern, i.e.  $f_0 = 0.125 \text{ pixels}^{-1}$ . The design of the FIR filter required by SDP is based on the observation that, as the distance between the low-frequency spectrum and the main unwanted spectra (centered at  $2f_0, -2f_0$ ) of the frequency-shifted signal is large, the transition from passband to stopband can be made smooth in order to optimize stopband attenuation. The designed filter is shown in the upper plot in Figure 2, where the frequency axis is normalized to  $f_0$ . Since the attenuation at  $2f_0$  and  $4f_0$  is respectively  $55.4 \text{ db}$  and  $28.5 \text{ db}$ , the unwanted spectra are adequately rejected and accurate profile reconstruction is expected. Figure 3 shows the reconstruction (dashed line) of the target phase profile (solid line) by FTP (upper plot) and SDP (lower plot). Due to the non-ideal stopband rejection of the FIR filter, the SDP profile is sharper and slightly noisy. Yet, simulation shows both techniques to be potentially accurate with fringe frequencies as high as  $0.125 \text{ pixels}^{-1}$ .

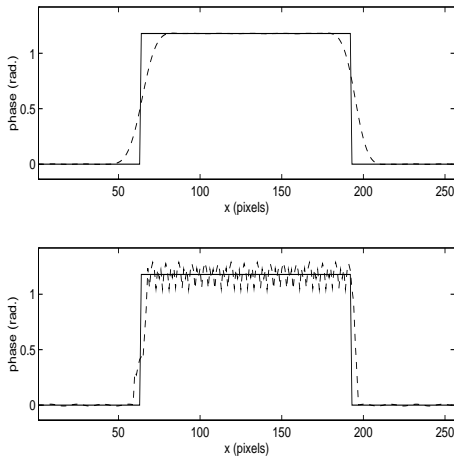


Figure 4: Profile reconstruction by FTP and SDP.

Then, we simulate the projection of the coarse fringe pattern, i.e.  $f_0 = 0.0625 \text{ pixels}^{-1}$ . With such a low fringe frequency, a sharp transition from passband to stopband is required to separate effectively the low-frequency spectrum from those centered at  $2f_0, -2f_0$ . Compared with the filter designed for the fine pattern, the transition should be made sharp enough to move point  $f_n = 1$ <sup>3</sup> outside the first lobe. The filter designed to fulfil this specification is shown in the lower plot in Figure 2, where the frequency axis is normalized with respect to the coarse pattern frequency. Figure 4 shows the reconstruction of the target phase profile<sup>4</sup> by FTP and SDP using the coarse pattern. In this case FTP is significantly more accurate. The Fourier transform of the SDP error with respect to the target profile reveals that the higher spectra ( $4f_0, 6f_0$ ) are not attenuated effectively by the filter. On the other hand, the rejection of higher spectra can be increased only by smoothing the transition from passband to stopband; as this moves the spectrum at  $2f_0$  - which is the main unwanted spectrum - into the first lobe of the filter, errors turn out to be larger.

Hence, with a coarse pattern, FTP straightforwardly enables tight extraction of the desired information while the design of the FIR filter required by SDP is problematic, the sharp transition needed to attenuate the main “noise” spectrum implying less effective attenuation of higher unwanted spectra. As a result, SDP is less accurate than FTP. When dealing with real images reflectivity is non-uniform and the contribution of the low-frequency spectrum is not eliminated by mean value subtraction. This makes the design of the SDP filter even more problematic. Consequently, SDP is expected to be significantly less accurate than FTP with real images and coarse patterns.

<sup>3</sup>The coarse pattern frequency is half the fine pattern one.

<sup>4</sup>The target phase step is half the one in Figure 3 because the phase step associated with a given height step depends on the grating period ( see [3]).

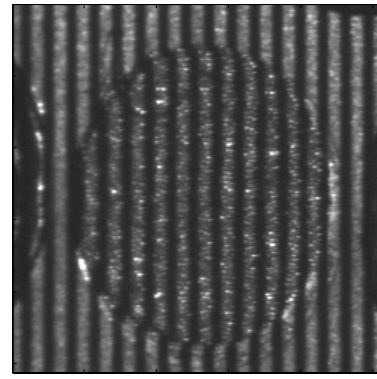


Figure 5: Pad on the PCB with the projected fringe pattern.

## 4 EXPERIMENTAL RESULTS

An optical bench has been set-up to evaluate FTP and SDP on a set of PCB samples provided by Motorola. Fringe generation-acquisition is obtained by a projector mounted vertically with respect to the bench and an angularly offset camera. The projector is made out of a fibre-optic white light source followed on the optical path by a Ronchi grating and a final focusing lens. An  $8 \text{ lines/mm}$  and a  $20 \text{ lines/mm}$  gratings were used in the experiments. Basically, the grating frequency establishes the fringes frequency at the object-level and the magnification associated with object-camera distance sets the actual frequency at the image level. It was found experimentally that the optical system needed to be adjusted carefully so as to obtain sharp fringe images. This was achieved by using the coarser of the available gratings and positioning the camera rather close to the object. Indeed, this configuration maximizes light transmission from the source to the object as well as from the object to the sensor. The adopted optical configuration is based on the  $8 \text{ lines/mm}$  grating and the fringe frequency at the image level is  $0.0625 \text{ pixels}^{-1}$ .

Figure 5 shows the image of a circular pad on the PCB with the projected fringe pattern. Fringes bend while crossing the pad because of the elevation with respect to the PCB surface associated with solder paste. This results in a phase difference between the image rows crossing the pad and those located at the flat PCB surface. Phase difference values can be translated into height values by a calibration process.

Figure 6 shows the phase map extracted using FTP: angles are mapped into gray-levels with darker points representing higher phase deviations ( i.e. heights ). FTP allows the elevation with respect to the PCB surface associated with the pad to be detected neatly. SDP is implemented using the filter shown in the lower plot in Figure 2, which is the best filter designed in the simulations for  $f_0 = 0.0625 \text{ pixels}^{-1}$ . The resulting phase map is shown in Figure 7. SDP reconstruction is less tidy and the presence of an oscillating component is visible. The

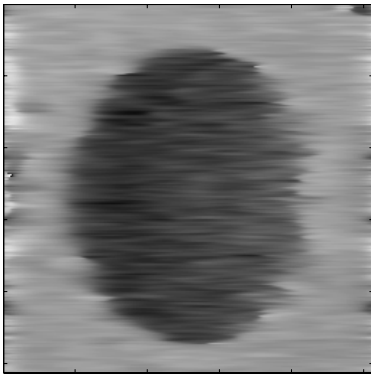


Figure 6: Phase map obtained by FTP.

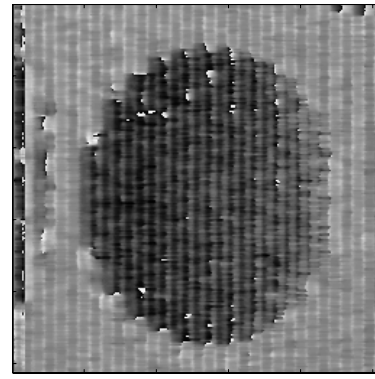


Figure 8: Phase map obtained by SDP.

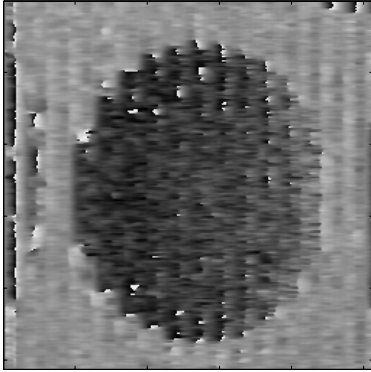


Figure 7: Phase map obtained by SDP.

Fourier transform of the SDP profile reveals that the oscillation is due to the spectrum centered at  $f_0$ . Indeed, the low-frequency spectrum of the image moves at  $f_0$  after the frequency-shifting step of SDP and falls in the first lobe of the filter. Trying to increase the rejection of the spectrum centered at  $f_0$  by sharpening the transition band of the filter causes stopband attenuation to decrease, the main source of error turning out to be a quasi-sinusoidal signal of frequency  $2f_0$ . The phase map obtained with a filter having a sharper transition band is shown in Figure 8

Hence, experimental results are consistent with simulation results. FTP allow neat detection of an elevation with respect to the PCB surface corresponding to the solder paste on pads. Since the optimal optical set-up relies on a coarse fringe pattern, the results achieved using SDP are not satisfactory.

## 5 CONCLUSIONS AND FUTURE WORK

We investigated the use of phase profilometry techniques for on-line solder paste inspection. In this paper we have reported on the comparison between Fourier Transform Profilometry and Signal Domain Profilometry.

Simulation results show that, in order to exploit SDP's higher speed, a high-frequency fringe pattern should be used. Instead, due to the basic requirement

of obtaining sharp fringe images, our optical set-up is based on a rather low frequency. According to simulation, FTP yields better experimental results than SDP, allowing neat detection of the elevation with respect to the PCB surface associated with solder paste on pads.

The major drawback of an on-line solder paste inspection system based on Fourier Profilometry is speed. In the second part of our work a new profilometry technique was devised. The technique, described in a paper under preparation, yields results very similar to FTP and is 20 times faster.

Due to the unavailability of reference solder paste height maps, we could not measure the actual accuracy of the techniques investigated. Thus, future work is aimed at quantitative assessment of accuracy of phase profilometry techniques.

## Acknowledgments

We wish to thank Richard Watson and Sean Ó Neill of Machine Vision Centre, Dublin, for their valuable help in the experimental part of this work.

## References

- [1] J. Jalkio. *Choosing Solder Paste Inspection Equipment*. Surface Mount Technology Magazine, September, 1995
- [2] J. Pearson, F. Lilley, D. Burton, et al. *Phase measuring methods for the measurement of three-dimensional shape in automated inspection of manufactured electronic assemblies*. Proceedings of the SPIE, Vol. 2183, 1994
- [3] M. Takeda, K. Mutoh. *Fourier transform profilometry for the automatic measurement of 3-D object shapes*. Applied Optics, Vol. 22, No. 24, December, 1983
- [4] M. Takeda, H. Ina, S. Kobayashi. *Fourier-transform method of fringe-pattern analysis for computer-based topography and interferometry*. Journal of the Optical Society of America, Vol. 72, No. 1, January, 1982
- [5] S. Tang, Y. Hung. *Fast profilometer for the automatic measurement of 3-D object shapes*. Applied Optics, Vol. 29, No. 20, July, 1990
- [6] I. Rabiner, J. McClellan, T. Parks. *FIR Digital Filter Design Using Weighted Chebyshev Approximations*. Proceedings IEEE, Vol. 63, 1975